# 行政院國家科學委員會專題研究計畫成果報告

## 對稱性突縮流場之流動分岐研究

## Bifurcations of flow through plane symmetric channel contraction

計畫編號：NSC90-2611-E-002-017

執行期限：90年8月1日至91年7月31日

主持人：蔣 德 普 國立台灣大學造船及海洋工程學系 教授

**Abstract**

Computational investigations have been performed into the behavior of an incompressible fluid flow in the vicinity of a plane symmetric channel contraction. The aim is to determine the critical Reynolds number, above which the flow becomes asymmetric with respect to the channel geometry using the bifurcation diagram. Three channels, which are characterized by the contraction ratio, are studied and the critical Reynolds numbers are determined as 3075, 1355 and 1100 for channels with contraction ratios of 2, 4, and 8, respectively.

**中文摘要**

以計算方法探討二維渠道流場因斷面對稱性突縮之流動分岐現象。渠道突縮比 $C=2$, 4 與 8 流場之臨界雷諾數經界定分別為 3075, 1355 與 1100。

### 1. Introduction

Several investigations have been performed in order to understand the incompressible flow downstream of a channel contraction, which is planar and is normal to the direction of the channel wall. These investigations have been both experimental, see, for example, Durst et al.[1], and numerical, for example, the works of Dennis and Smith[2], Hunt[3], Hawken et al.[4] and Huang and Seymour[5]. The above cited stream function-vorticity analyses employed different ways of avoiding the infinite vorticity at the sharp corners. Investigations into this channel flow allow better understanding of flow separation, which are common features in engineering practice. As a result, we conduct here a parametric study by varying the Reynolds numbers and the contraction ratios.

When conducting experiments for the flow downstream of a plane, symmetric channel expansion, Cherdron et al.[6] and Sobey[7] observed a larger recirculation region which appeared preferentially at one wall of the channel, thus indicating the existence of a critical Reynolds number, $Re_c$, above which the flow becomes substantially different from that observed below this value. When the flow is no longer symmetric about the centerline of the channel, a process known as pitchfork bifurcation has been found to occur. Under these circumstances, momentum transfer proceeds between the fluids shear layers. This transfer in momentum, in turn, causes a pressure gradient to form across the channel. Such a pressure gradient may lead to an asymmetric flow. We refer to this phenomenon as the Coanda effect (Wille and Fernolz[8]). Numerical simulation of the contraction flow in geometrically symmetric channels has been conducted mostly in a half domain[1-3,5]. In this paper, we address the bifurcation flow in the full domain.

### 2. Mathematical model

In the present investigation, we simulated the flow of an incompressible fluid through a 2-D contraction channel. Referring to Fig. 1, the governing equations for simulating this channel flow can be expressed in vector form as:

$$\underline{u}\cdot\nabla\underline{u}=-\nabla p+\frac{1}{Re}\nabla^2\underline{u}, \qquad (1)$$

$$\nabla\cdot\underline{u}=0. \qquad (2)$$

In the above equations, $u$ and $v$ are the components of the velocity vector $\underline{u}$ in the $x$

and $y$ directions, respectively, and $p$ is the static pressure. These primitive variables have been normalized by dividing $u$ and $v$ by the inlet mean velocity, $U_{\text{mean}}$, and $p$ by $\rho U_{\text{mean}}^2$, where $\rho$ is the fluid density. The independent variables are normalized by the upstream channel height $D$, leading to the Reynolds number, $Re = \frac{\rho U_{\text{mean}} D}{\mu}$, where $\mu$ denotes the dynamic viscosity.

Upstream of the step plane, the fluid enters the channel at $x$ = -2.5, at which a fully developed velocity profile is prescribed as $\underline{u}$ = (6(0.5+$y$)(0.5-$y$), 0). The channel exit is considered to be sufficiently far from the step to allow the flow to have a zero gradient velocity profile. Given this assumption we prescribe zero gradient velocity vector at $x$ = 5. The no-slip velocity condition is, as a usual, prescribed on the solid walls. The present primitive-variable formulation can avoid dealing with the corner singularity, which is encountered in the stream function-vorticity formulation.

## 3. Numerical model

Working equations (1-2) are integrated in their respective finite volume, each of which are associated with a particular primitive variable and is placed on the centroid of the finite volume. A serious problem, which has been encountered when simulating incompressible Navier-Stokes equations, is checkerboard pressure oscillations. To overcome this difficulty, field variables are stored at staggered grids (Table 1). Numerical simulation of incompressible Navier-Stokes equations entails another instability, which is evident from the oscillatory velocities, when dominated advective terms are discretized using centered schemes. The loss of convective stability is particularly pronounced in multi-dimensional flow simulations. To fix this problem, we have modified the QUICK scheme of Leonard[9] and implemented it in non-uniform grids to resolve this instability problem and avoid the false diffusion error. Discretization of other derivatives is performed using the centered-scheme for revealing their elliptic characters.

In solving the finite volume discretized equations for (1-2), we abandon the coupled approach due to the need for much more disk storage space compared to the space needed when solving these equations separately by the SIMPLE-C solution algorithm (Van Doormaal and Raithby[10]). Use of this algorithm has been found to produce accurate results with a good rate of convergence. The pressure field is solved using the pressure correction method. In the staggered meshes, there are no storage points for the pressure at the domain boundary. Specification of pressure boundary conditions is not needed. In all the cases investigated, the solution was said to have converged when the global $L_2$-norm of pressure and velocity residuals reached a value below $10^{-15}$. Besides this stringent convergence requirement, it is also demanded that the relative difference of mass flux between the inlet and other arbitrarily chosen cross sections be less than $10^{-10}$.

## 4. Numerical results

In the present investigation, a computer code was run to simulate the fluid flow through three channels, each of which contains a plane symmetric contraction. The channel geometry is characterized by the dimensionless contraction ratio $C$ = 2, 4, 8. Reynolds numbers in the wide range of $0.1 \le Re \le 4000$ for the case of $C$ = 2 and in the range of $0.1 \le Re \le 2000$ for cases $C$ = 4, 8 were considered in order to allow us to study the Coanda effect.

### 4.1 Half-domain computation

Separation in a contraction channel can be characterized by the recirculation eddies at the upstream salient corner and downstream tip corner. It is, thus, important to select controlling parameters that could well characterize the flow separation. We choose the separation length $L_1$ and re-attachment length $L_2$ in a salient corner. While the tip corner separation length existed, its value was too small to be considered. Therefore, only the re-attachment length $L_3$ is considered in the tip corner. Varying the Reynolds number and the contraction ratio does investigations. To begin with, calculations were carried on the half channel by imposing the symmetric boundary condition at the centerline $y = 0$ in order to obtain symmetric solutions. These half-domain solutions will be compared with those computed in the full channel for clarifying the presence of bifurcation solutions.

The separation/reattachment lengths $L_1$ and $L_2$ of the upstream salient corner eddy are plotted logarithmically against the Reynolds number as shown in Fig. 2. It is shown that $L_1$ tends to have a constant value, which is smaller than that of $L_2$ as $Re$ decreases from $10^0$ to $10^{-1}$. As $Re > 10^0$, lengths $L_1$ and $L_2$ are prone to decrease, with the length $L_2$ being largely decreased. This implies that $L_1$ has a tendency to reach the value of $L_2$ as $Re$ approaches to $10^1$. A further increase of $Re$ causes $L_1$ to have a value larger than $L_2$. When the Reynolds number is further increased up to $10^2$, both lengths $L_1$ and $L_2$ increase with $Re$. The $L_1$ increases at a larger slope. When the Reynolds number becomes larger than $10^1$, $L_1$ is still larger than $L_2$.

The downstream tip corner eddy becomes visible as the Reynolds number increases up to Re $\sim 10^2$. The results shown in Fig. 3 reveal that the tip corner reattachment length $L_3$ varies linearly with the Reynolds number according to $L_3 = a * Re - b$, where $(a, b) =$ $(0.336\times10^{-3}, 0.109)$ , $(0.401\times10^{-3}, 0.056)$ and $(0.258\times10^{-3}, 0.032)$ for $C = 2$, 4 and 8, respectively.

### 4.2 Full-domain computation

For clarifying the presence of the well-known pitchfork bifurcation in contraction channel, we conducted analysis on the entire channel. To provide a measure of flow asymmetry, we subtract the half-domain solutions from the full-domain solutions for the lengths $L_1$, $L_2$, and $L_3$. The resulting lengths $\Delta L_1$, $\Delta L_2$, and $\Delta L_3$ are normalized by those obtained on the basis of half-domain analysis. We tabulate $L_i$ and $\Delta L_i / L_i$ by varying the Reynolds number and the contraction ratio in Table 2. The results reveal that when the value of $Re$ is lower than 2800, 1200, and 1000 for $C = 2$, 4, and 8, respectively, there exists a stable flow in which the recirculating eddies have the same size on the roof/floor of the channel. Under the circumstances, solutions compare favorably with half-domain solutions in the sense that the difference between two sets of data is less than 0.1% for lengths $L_1$ and $L_2$ and 1% for length $L_3$. This is not the case as $Re$ continuously increases, in particular for the reattachment length $L_3$. The difference between half- and full-domain calculations can be as high as 1% for $L_1$ and $L_2$ and over 20% for $L_3$ as the value of $Re$ is larger than 3200, 1400, and 1200 for $C = 2$, 4, and 8, respectively.

Note that the critical Reynolds numbers for pitchfork bifurcation fall into the ranges of $2800 < Re < 3200$ , $1200 < Re < 1400$ , and $1000 < Re < 1200$ for $C = 2$, 4, and 8, respectively. The larger the contraction ratio, the easier the bifurcation sets in. In this study, we plot the value of $L_3$ on the channel roof /floor from solutions computed in the full channel to determine critical Reynolds numbers. We then determine the intersection point of the resulting parabola, as shown in Fig. 3, with the line computed under the half-domain calculations. The critical Reynolds numbers are obtained as 3080, 1350, and 1100 for channels with $C = 2$, 4, and 8, respectively.

Other measures of the flow asymmetry and the critical Reynolds number can be obtained by computing the asymmetry-energy, $I = \int_0^{x_{max}} v^2\big|_{y=0} dx$, along the centerline of the channel. It can be seen from Fig. 4 the bifurcation diagram, obtained on the basis of the asymmetry-energy, that the value of $I$ is a nominal zero below the critical Reynolds number. Above the critical Reynolds number, at which the so-called pitchfork bifurcation appears, the flow apparently becomes asymmetric in the sense that $I$ increases by a factor of $10^2 \sim 10^3$ times of that below the critical value. At the critical points seen in Fig. 4, $dI/dRe$ takes the maximum value. This implies that ahead of the critical point $d(dI/dRe)/dRe < 0$ while behind the critical point $d(dI/dRe)/dRe > 0$. The critical Reynolds numbers determined in this way are 3070, 1360, and 1100 for channels with $C$ = 2, 4, and 8, respectively. A comparison of Figs. 3 and 4 reveals that critical Reynolds numbers determined by the above two means are, in essence, identical. It can be concluded that $Re$ = 3075, 1355 and 1100 (obtained from the mean value of two criteria) are the critical Reynolds numbers for channels with $C$ = 2, 4 and 8, respectively.

## 5. Concluding remarks

Computational investigations have been performed to study flow bifurcation in the symmetric planar contraction channel. The results obtained at different channel contraction ratios and Reynolds numbers clearly confirm that the pitchfork bifurcation can be present. Asymmetric solutions, manifested by unequal tip corner reattachment lengths at the channel floor/roof, can be stably maintained in cases when the Reynolds number exceeds its critical value. Another way to determine the critical Reynolds number is to plot the asymmetry-energy along the centerline of the channel for each investigated Reynolds number.

## References


1. Durst, F., Schierholz, W. F., and Wunderlich, A. M., 1987, "Experimental and numerical investigations of plane duct flows with sudden contraction," ASME *Journal of Fluids Engineering*. Vol. 109, pp. 376-383.
2. Dennis, S. C. R., and Smith, F. T., 1980, "Steady flow through a channel with a symmetrical constriction in the form of a step," *Proceedings of the Royal Society, London*, Series A372, pp. 393-414.
3. Hunt, R., 1990, "The numerical solution of the laminar flow in a constricted channel at moderately high Reynolds number using Newton iteration," *International Journal for Numerical Methods in Fluids*, Vol. 11, pp. 247-259.
4. Hawken, D. M., Townsend, P., and Webster, M. F., 1991, "Numerical simulation of viscous flows in channels with a step," *Computers & Fluids*, Vol. 20, pp. 59-75.
5. Huang H., and Seymour, B. R., 1995, "A finite difference method for flow in a constricted channel," *Computers & Fluids*, Vol. 24, pp. 153-160.
6. Cherdron, W., Durst, F., and Whitelaw, J. H., 1978, "Asymmetric flows and instabilities in symmetric ducts with sudden expansions," *Journal of Fluid Mechanics*, Vol. 84, pp. 13-31.
7. Sobey, I. J., 1985, "Observation of waves during oscillating channel flow," *Journal of Fluid Mechanics*, Vol. 151, pp. 395-426.
8. Wille, R. and Fernholz, H., 1965, "Report on the first European Mechanics Colloquium, on the Coanda effect," *Journal of Fluid Mechanics*, Vol. 23, pp. 801-819.
9. Leonard, B. P., 1979, "A stable and accurate convective modeling procedure based on quadratic upstream interpolation," *Computer Methods in Applied Mechanics and Engineering*, Vol. 19, pp. 59-98.
10. Van Doormaal J. P., and Raithby, G. D., 1984, "Enhancements of the SIMPLE method for predicting incompressible fluid flows," *Numerical Heat Transfer*, Vol. 7, pp.147-163.


Table 1. Grid details

| $C$ | N-$\Delta x$ | N-$\Delta y$ | $(\Delta x_{min}, \Delta x_{max})$ | $(\Delta y_{min}, \Delta y_{max})$ |
|---|---|---|---|---|
| 2 | 110 | 130 | (0.001, 0.25) | (0.0005, 0.022) |
| 4 | 110 | 180 | (0.001, 0.25) | (0.0005, 0.010) |
| 8 | 110 | 180 | (0.001, 0.25) | (0.0005, 0.008) |

Table 2. The computed separation and reattachment lengths. (a) the computed symmetric solution in a half-channel. (b) and (c) reveal bifurcated solutions, in percentage difference relative to (a), in the full-channel computation.

| $C$ | $Re$ | $L_1$ (a) | $L_1$ (b) | $L_1$ (c) | $L_2$ (a) | $L_2$ (b) | $L_2$ (c) | $L_3$ (a) | $L_3$ (b) | $L_3$ (c) |
|---|---|---|---|---|---|---|---|---|---|---|
| 2 | 1000 | 0.140 | 0.0% | +0.1% | 0.078 | 0.0% | +0.1% | 0.228 | 0.0% | +0.7% |
| | 2000 | 0.181 | 0.0% | +0.1% | 0.089 | 0.0% | +0.1% | 0.562 | 0.0% | +0.6% |
| | 2800 | 0.204 | 0.0% | +0.1% | 0.096 | 0.0% | +0.1% | 0.834 | -0.6% | +1.1% |
| | 3200 | 0.212 | -0.5% | +0.6% | 0.098 | -0.2% | +0.3% | 0.969 | -22.2% | +21.9% |
| | 3600 | 0.219 | -1.1% | +1.2% | 0.099 | -0.5% | +0.5% | 1.103 | -38.7% | +36.6% |
| | 4000 | 0.227 | -1.3% | +1.4% | 0.100 | -0.6% | +0.6% | 1.237 | -46.2% | +40.4% |
| 4 | 500 | 0.157 | 0.0% | 0.0% | 0.097 | 0.0% | 0.0% | 0.146 | 0.0% | +0.7% |
| | 1000 | 0.202 | 0.0% | 0.0% | 0.112 | 0.0% | 0.0% | 0.343 | -0.1% | +0.8% |
| | 1200 | 0.214 | 0.0% | 0.0% | 0.116 | 0.0% | 0.0% | 0.423 | -0.6% | +1.2% |
| | 1400 | 0.225 | -0.3% | +0.3% | 0.119 | -0.2% | +0.3% | 0.504 | -20.5% | +19.5% |
| | 1700 | 0.239 | -0.6% | +0.6% | 0.123 | -0.4% | +0.4% | 0.626 | -45.6% | +37.6% |
| | 2000 | 0.250 | -0.6% | +0.7% | 0.126 | -0.4% | +0.5% | 0.749 | -53.9% | +37.4% |
| 8 | 400 | 0.156 | 0.0% | 0.0% | 0.100 | 0.0% | 0.0% | 0.073 | 0.0% | +1.0% |
| | 700 | 0.194 | 0.0% | 0.0% | 0.112 | 0.0% | 0.0% | 0.148 | -0.1% | +0.8% |
| | 1000 | 0.217 | 0.0% | 0.0% | 0.120 | 0.0% | 0.0% | 0.224 | -0.8% | +1.2% |
| | 1200 | 0.231 | -0.3% | +0.3% | 0.124 | -0.2% | +0.2% | 0.275 | -33.0% | +29.5% |
| | 1500 | 0.246 | -0.3% | +0.3% | 0.130 | -0.2% | +0.2% | 0.354 | -51.2% | +36.9% |
| | 2000 | 0.267 | -0.4% | +0.4% | 0.135 | -0.3% | +0.3% | 0.485 | -62.6% | +28.4% |

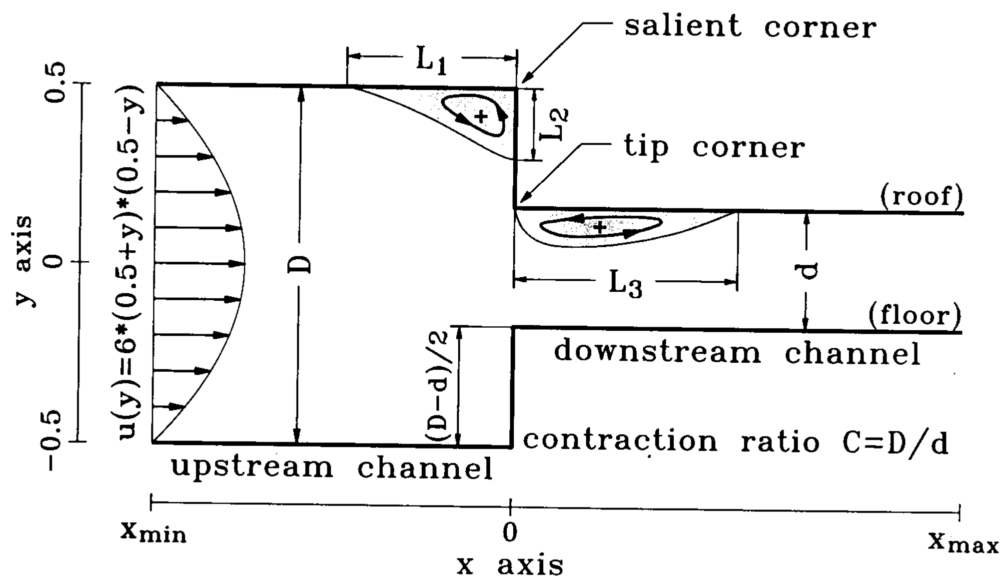


Fig. 1 The geometry and controlling lengths that can characterize the flow reversal in the contraction channel.

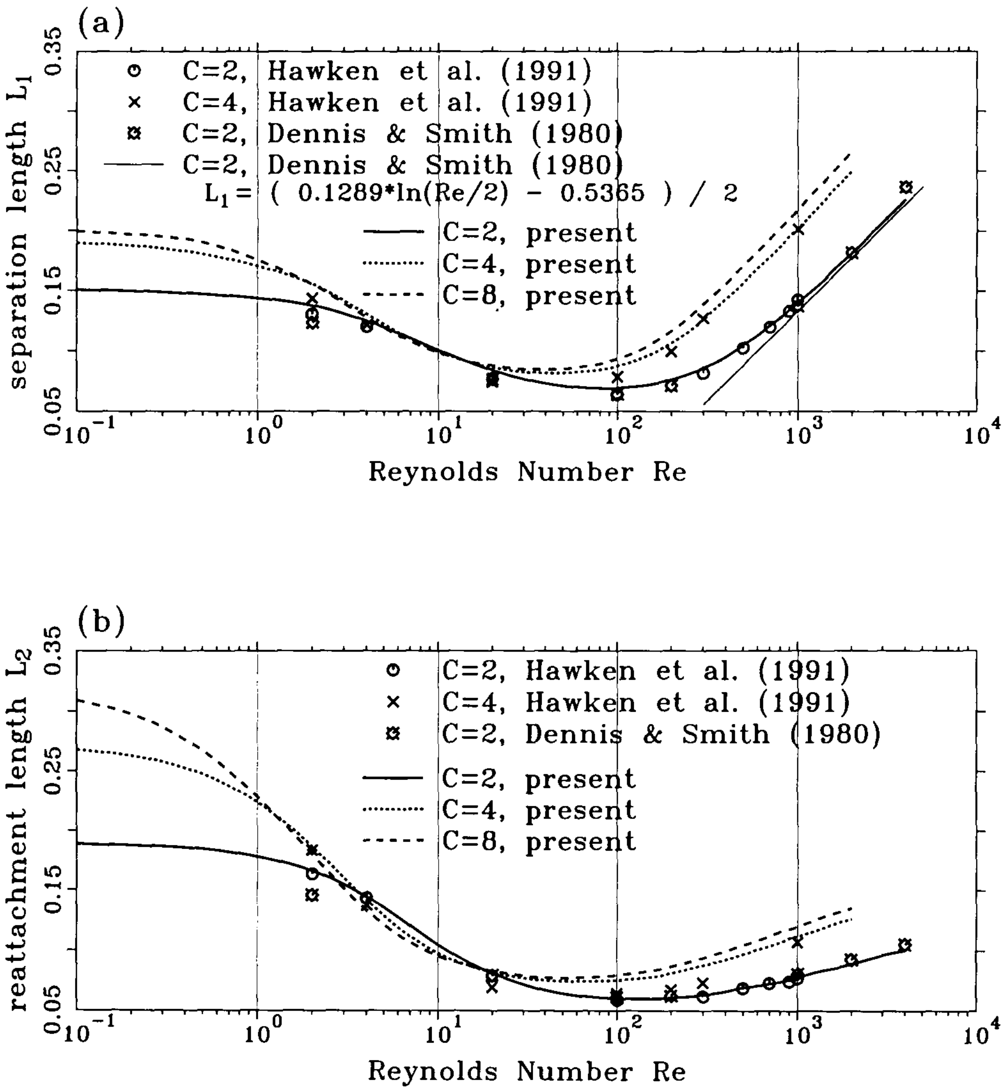


Fig. 2 A comparison of separation/reattachment lengths of upstream salient corner eddy between the present calculation and other numerical data for $C = 2, 4, 8$ at different Reynolds numbers. (a) separation length $L_1$; (b) reattachment length $L_2$.

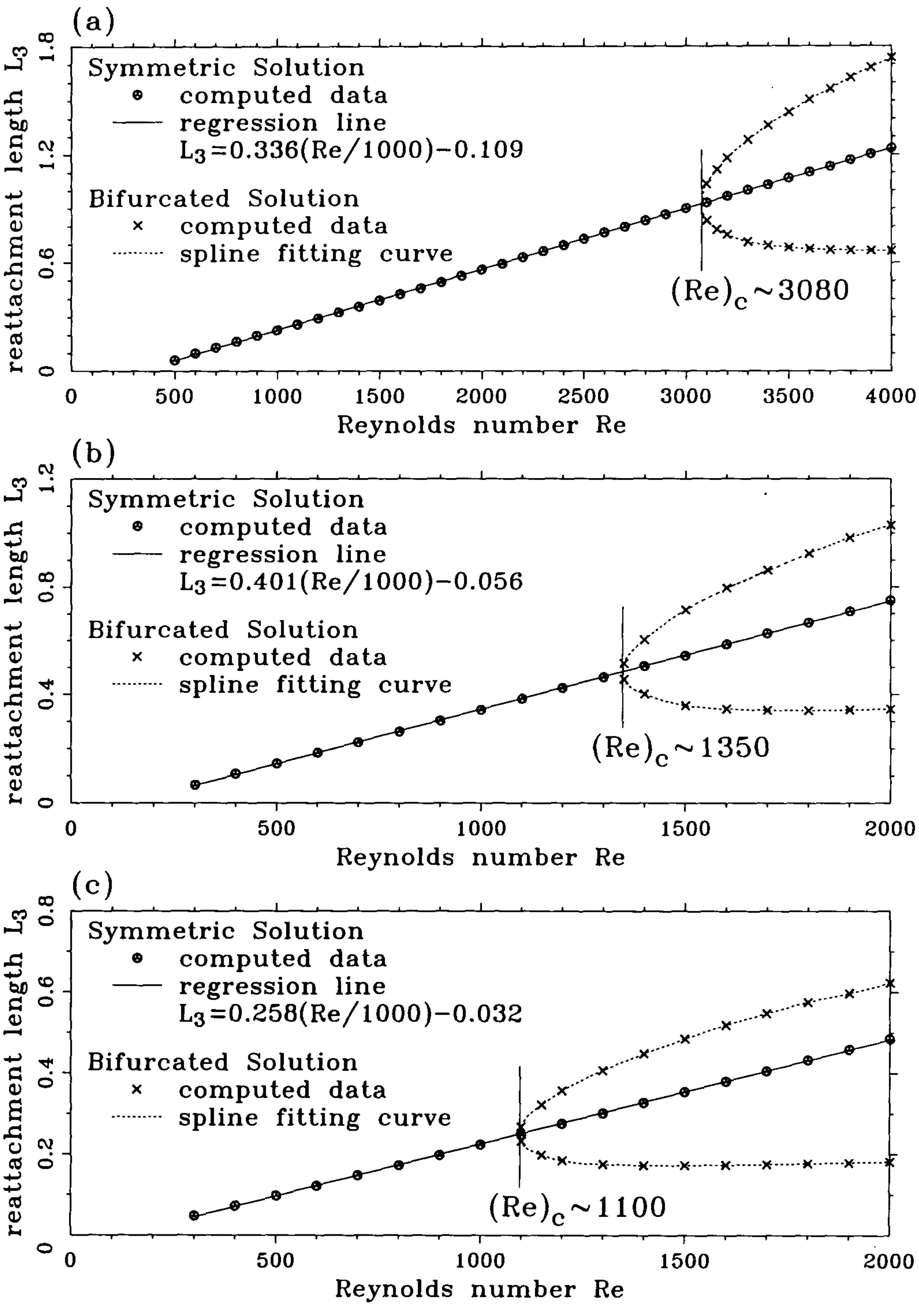


Fig. 3 The plot of reattachment lengths $L_3$ of downstream tip corner eddy against Reynolds numbers. (a) $C = 2$; (b) $C = 4$; (c) $C = 8$.

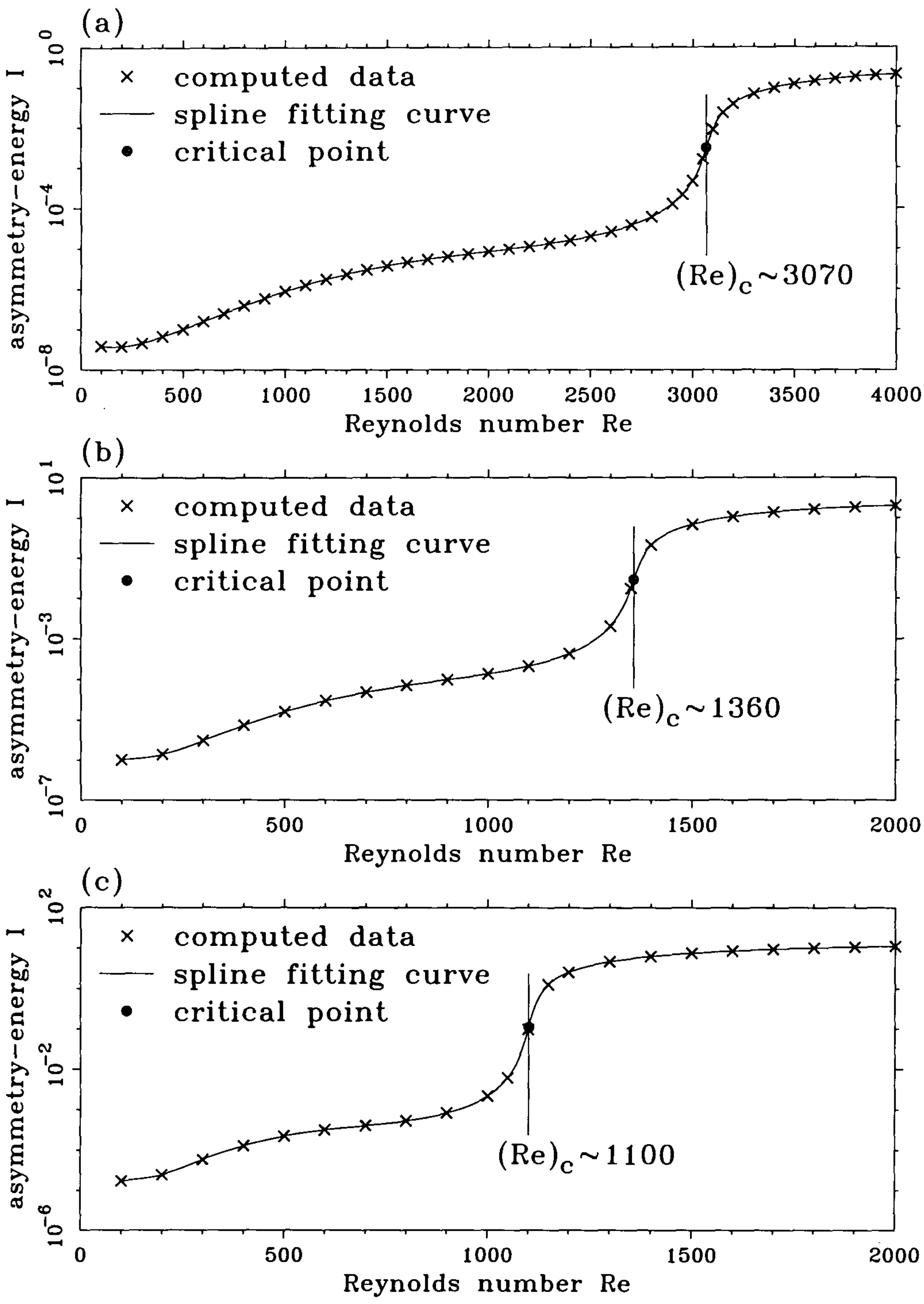


Fig. 4 The plot of asymmetry-energy values against Reynolds numbers in channels of different contraction ratios. (a) $C = 2$; (b) $C = 4$; (c) $C = 8$.